Accepted to AJ: 2007 May 22
Preprint typeset using LaTeX style emulateapj v. 03/07/07

FRACTION OF CONTACT BINARY TROJAN ASTEROIDS

Rita K. Mann, David Jewitt & Pedro Lacerda
Institute for Astronomy, University of Hawaii, 2680 Woodlawn Drive, Honolulu, HI 96822

(Received 2006 October 6)
Accepted to AJ: *2007 May 22*

ABSTRACT

We present the results of an optical lightcurve survey of 114 Jovian Trojan asteroids conducted to determine the fraction of contact binaries. Sparse-sampling was used to assess the photometric range of the asteroids and those showing the largest ranges were targeted for detailed follow-up observations. This survey led to the discovery of two Trojan asteroids, (17365) and (29314) displaying large lightcurve ranges ($\sim$ 1 magnitude) and long rotation periods ($<$ 2 rotations per day) consistent with a contact binary nature. The optical lightcurves of both asteroids are well matched by Roche binary equilibrium models. Using these binary models, we find low densities of $\sim$ 600 kg m^{-3} and 800 kg m^{-3}, suggestive of porous interiors. The fraction of contact binaries is estimated to be between 6% and 10%, comparable to the fraction in the Kuiper Belt. The total binary fraction in the Trojan clouds (including both wide and close pairs) must be higher.

Subject headings: minor planets — asteroids — solar system: general — surveys

1. INTRODUCTION

The existence and importance of binary asteroids in small-body populations has only been realized in the last decade, after the first unambiguous detection of a satellite around main-belt asteroid 243 Ida by the Galileo spacecraft (Belton et al. 1995; Chapman et al. 1995). It is now evident that binaries exist in the main-belt asteroids, the near-earth asteroids and in the Kuiper Belt (see review by Richardson & Walsh (2006) and references therein). Apart from spacecraft flybys (and the rare case of measuring gravitational perturbations of planets by very large asteroids), studying the orbital dynamics of binary systems provides the only method available for calculating mass and density. Density measurements are important as probes of internal structure, enabling constraints to be placed on the porosity and composition.

The Jovian Trojan asteroids are trapped in a 1:1 mean motion resonance with Jupiter. They form two large clouds around the stable (L4, L5) Lagrangian points 60° ahead of and behind the giant planet. It has been estimated that $\sim 10^5$ Trojan asteroids with diameters larger than 1-km exist (Jewitt, Trujillo, & Luu 2000; Yoshida & Nakamura 2005), comparable in number to the Main Belt population (6.7×10^5 asteroids, Ivezic et al. (2001)), making it clear that they comprise an important reservoir of information. The Trojan asteroids of Jupiter have yet to be searched systematically for the presence of binaries. Despite this fact, two Trojan binaries have already been identified: 617 Patroclus, a resolved wide binary discovered by Merline et al. (2001), while 624 Hektor has a distinctive lightcurve that indicates it is a close or contact binary (Cook (1971), Hartmann et al. (1988)) and a widely separated satellite has recently been imaged (Marchis et al. 2006b). The Trojans are intriguing because they show larger photometric ranges when compared with main-belt asteroids (Hartmann et al. 1988), particularly those with diameters larger than 90-km (Binzel & Sauter 1992). Large lightcurve amplitudes suggest elongated shapes or binarity.

While it is not clear whether the Trojans formed at their current location alongside Jupiter or were trapped after forming at larger heliocentric distances (Morbidelli et al. 2005), it is believed that these bodies are primordial. Understanding their composition and internal structure is therefore of great interest, making density determination vital. The density of Trojan 617 Patroclus has been estimated as $\rho = 800^{+200}_{-100}$ kg m^{-3} based on the measured orbital period and size, and on diameter determinations made from infrared data (Marchis et al. 2006a). This low density contrasts with a comparatively high estimate for 624 Hektor, namely $\rho = 2480^{+290}_{-80}$ kg m^{-3}, determined from the lightcurve and a Roche binary model (Lacerda & Jewitt 2007).

Close or contact binaries are composed of two asteroids in a tight orbit around each other. The Trojan contact binary fraction is potentially important in distinguishing between various formation theories. For example, one model of binary formation by dynamical friction predicts that close binaries should be common (Goldreich, Lithwick, & Sari 2002) while another based on 3-body interactions asserts that they should be rare (Weidenschilling 2002). The nature of the Trojan binaries can also reveal clues about their formation. It is known that different mechanisms formed binaries in the Main Belt and the Kuiper Belt because of the distinct types of binaries found in both populations. It is suspected that gravitational processes predominantly form Kuiper Belt binaries, the known examples of which have components of comparable mass and large separations (Weidenschilling 2002; Goldreich, Lithwick, & Sari 2002; Funato et al. 2004; Astakhov, Lee, & Farrelly 2005). Sub-catastrophic impacts followed by gravitational interaction with the debris formed are the leading way to form tight binary systems with unequal mass components that make up the larger main-belt binary population (Weidenschilling 1989; Richardson & Walsh 2006). A comparative study

Electronic address: rmann@ifa.hawaii.edu, jewitt@ifa.hawaii.edu, pedro@ifa.hawaii.edu

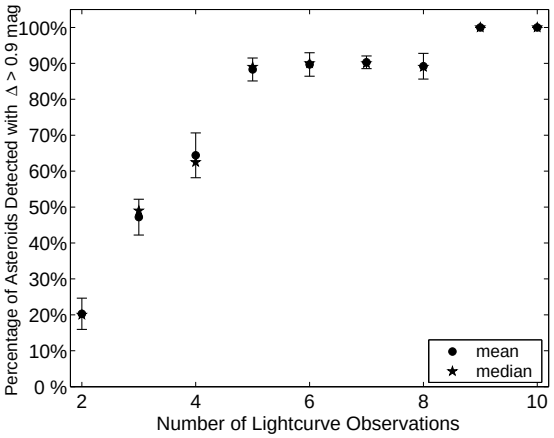

FIG. 1.— Percentage of asteroids detected with photometric ranges greater than 0.9 magnitudes versus number of lightcurve observations. Monte Carlo simulations were conducted on a sample of asteroids with a photometric range of 1.2 magnitudes and single-peaked lightcurve periods between 3 and 10 hours to determine sparse sampling efficiency.

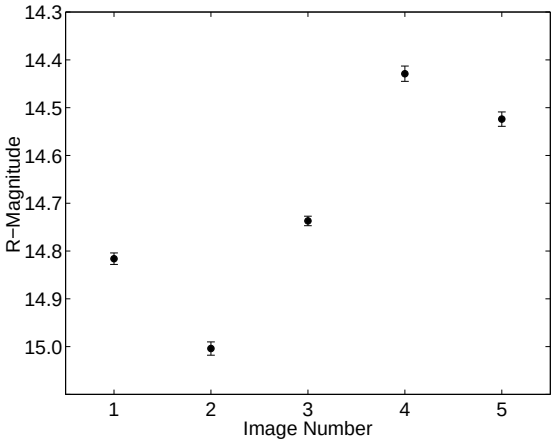

FIG. 2.— Sparse-sampled R-band photometry of 944 Hidalgo. The photometric range estimated from five observations is 0.58 ± 0.02 magnitudes, consistent with previous measurements of 0.60 magnitudes from Harris et al. (2006).

of the binaries in the Trojan clouds, the Main Belt and the Kuiper Belt might illuminate the different roles played by formation conditions in these populations.

Motivated by the lack of studies about Trojan binaries, the aim of this paper is to investigate the fraction of close or contact binary systems among the Jovian Trojan population. Contact binaries are specifically targeted for the ease with which they can be identified using optical lightcurve information. Here, we present a technique called sparse sampling, which we used to conduct a lightcurve survey of 114 Jovian Trojan asteroids. The results of this survey, the discovery of two suspected contact binary asteroids and a discussion of the binary fraction in the Jovian Trojan population will follow.

2. OBSERVATIONS

2.1. *Sparse Sampling*

The maximum photometric range that can be exhibited by a rotationally elongated, strengthless body is 0.9 mag (Leone et al. 1984). Ranges larger than 0.9 mag. are strongly suggestive of a contact binary nature, in which mutual gravitational deformation of the components can drive the range up to $\sim$ 1.2 magnitudes (Weidenschilling 1980; Leone et al. 1984). In principle, structurally strong bodies can maintain any shape and show an arbitrarily large photometric range. However, most main-belt asteroids larger than $\sim$ 150-m in diameter show little sign of possessing internal strength sufficient to resist gravity and/or rotational deformation (Pravec, Harris, & Michalowski 2002; Holsapple 2004) and we expect that the Trojan asteroids are similarly structurally weak. In what follows, we assume that objects with photometric range >0.9 mag. are candidate contact binaries.

To examine the efficiency of sparse lightcurve sampling, we conducted a series of Monte Carlo tests. The tests were applied to asteroids with a photometric range of 1.2 magnitudes and double-peaked lightcurve periods uniformly distributed between 6 and 20 hours. The lightcurves were uniformly sampled by N=1,2...10 observations over one night. Asteroids for which the sparse-sampling technique detected photometric ranges between 0.9 and 1.2 magnitudes were picked out as successful candidates. Monte Carlo simulations suggest that between 85% and 92% of asteroids with photometric ranges of 1.2 magnitudes would be identified as contact binary candidates from just five measurements of brightness per night (see Figure 1). (The efficiency of detecting brightness variations larger than 0.9 magnitudes ranged from $\sim$ 71% for asteroids with actual peak-to-peak lightcurve amplitudes of 1.0 magnitudes to $\sim$ 81% of asteroids with peak-to-peak amplitudes of 1.1 magnitudes.) The simulations indicate that the accuracy with which contact binary candidates are identified varies little when sampling between five and eight lightcurve points per asteroid (see Figure 1). The advantage of sparse sampling is clear: estimates of photometric range for a large number of asteroids can be made rapidly, significantly reducing observing time. Asteroids exhibiting large photometric ranges in the sparse sampling study are subsequently targeted for detailed follow-up observations with dense coverage in rotational phase space.

To further test the sparse sampling technique, we observed 2674 Pandarus and 944 Hidalgo, two asteroids known to show large photometric variations. From published lightcurves, 2674 Pandarus is known to have a photometric range of 0.49 magnitudes (Hartmann et al. 1988). Using the sparse sampling technique, with the same sampling as for all other asteroids in the study (and without prior knowledge of the rotational phase), we measured a lightcurve amplitude of 0.50 ± 0.01 magnitudes for Pandarus. Hidalgo has shown a maximum photometric variation of 0.60 magnitudes (Harris et al. 2006), whereas sparse sampling measured the brightness range to be 0.58 ± 0.02 magnitudes (see Figures 2 and 3). The agreement results show that the photometric range can be usefully estimated with only five measurements of asteroid brightness.

Having gained confidence in the technique through simulations and observational tests, we applied sparse sampling to the Trojan asteroids. Taking five short exposures, while cycling through the asteroids, we were able to obtain limited sampling of 114 asteroid lightcurves in nine good weather nights of observing.

2.2. *Data Acquisition and Reduction*

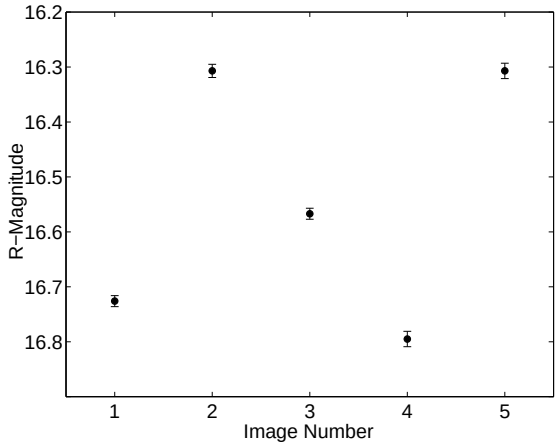

FIG. 3.— Sparse-sampled R-band photometry of 2674 Pandarus. The photometric range estimated from five observations is 0.50 ± 0.01 magnitudes, consistent with previous measurements of 0.49 magnitudes (Hartmann et al. 1988).

We obtained sparsely sampled optical lightcurve data for the Jovian Trojan asteroids using both the University of Hawaii 2.2-m telescope on Mauna Kea and the Lulin One-meter Telescope (LOT) in Taiwan. We used a 2048 x 2048 pixel Tektronix charge-coupled device (CCD) on the 2.2-m telescope. This detector has a 0.219 arcseconds per pixel image scale and a field of view of 7.5 square arcminutes. The CCD on LOT (VersArray:1300B) has 1340 x 1300 pixels with 0.516 arcseconds per pixel scale, and a field of view of 11.5 x 11.2 arcminutes. All images were taken in the R band with exposure times scaled to the brightnesses of the asteroids. On LOT, the exposure times ranged from 30 seconds for objects brighter than 15th magnitude, up to 120 seconds for 19th magnitude Trojans. At the 2.2-m telescope, the exposure times ranged from 10 seconds for objects brighter than 17th magnitude, to 150 seconds for 20th magnitude asteroids. See Table 1 for a description of the observations.

TABLE 1
JOURNAL OF OBSERVATIONS

UT Date	Telescope	Seeing (″)	Project[a]	Full/Half Night	Comments
2005 March 07	LOT 1-m	2.0	Sparse	Full	Scattered Cirrus
2005 March 09	LOT 1-m	2.2	Sparse	Full	Windy
2005 March 11	LOT 1-m	2.0	Sparse	Half	Cloudy
2005 March 13	LOT 1-m	1.7	Sparse	Full	Clear Skies
2005 April 05	UH 2.2-m	0.6	Sparse	Full	Cirrus
2005 April 06	UH 2.2-m	0.6-0.8	Sparse	Half	Cloudy
2005 April 07	UH 2.2-m	0.6	Sparse	Half	Photometric
2005 April 09	UH 2.2-m	0.6-0.7	Sparse	Half	Clear
2005 April 11	UH 2.2-m	0.6	Sparse	Half	Clear
2005 April 12	UH 2.2-m	0.7	Sparse	Half	Clear
2005 April 14	UH 2.2-m	0.7	Sparse	Half	Clear
2005 April 15	UH 2.2-m	0.8	Sparse	Half	Cloudy
2005 April 17	UH 2.2-m	0.8	Dense	Half	Cloudy
2005 April 18	UH 2.2-m	0.8-1.0	Dense	Half	Moon Rising
2006 February 01	UH 2.2-m	1.0	Dense	Full	Focus Problems
2006 February 02	UH 2.2-m	0.6	Dense	Full	Clear
2006 February 04	UH 2.2-m	1.5	Dense	Full	Strong Winds
2006 February 24	UH 2.2-m	1.0-1.2	Dense	Full	Windy
2006 April 24	UH 2.2-m	0.7	Dense	Half	Cloudy/Clear
2006 April 29	UH 2.2-m	0.8	Dense	Half	Clear,Windy
2006 April 30	UH 2.2-m	0.9	Dense	Half	Clear,Windy
2006 May 01	UH 2.2-m	0.9-1.0	Dense	Half	Windy

[a] Sparse Sampling Survey or Follow-up Densely Sampled Lightcurves

TABLE 2
PHOTOMETRY OF JOVIAN TROJAN ASTEROIDS

Trojans	Tel	$\bar{m}_R$[a]	$m_1 - \bar{m}_R$[b]	$m_2 - \bar{m}_R$[b]	$m_3 - \bar{m}_R$[b]	$m_4 - \bar{m}_R$[b]	$m_5 - \bar{m}_R$[b]	Δm_R[c]
884	UH	16.37	0.13	-0.09	-0.07	0.08	-0.05	0.22
1172	UH	15.78	0.06	-0.05	-0.04	0.03		0.11
1173	LOT	16.85	0.02	-0.20	-0.08	0.17	0.10	0.37
1208	UH	16.60	0.06	0.06	-0.01	0.00	-0.06	0.12
1583	UH	16.87	-0.02	-0.07	0.00	0.04	0.04	0.11
1647	UH	18.88	-0.20	-0.14	0.09	0.24		0.44
1867	UH	15.82	0.04	0.04	0.02	-0.07	-0.04	0.12
1868	UH	17.52	0.03	-0.03	-0.08	0.06	0.02	0.14
1869	UH	19.51	-0.18	0.01	0.03	0.07	0.08	0.26
1870	UH	17.90	-0.05	-0.01	0.05	-0.03	0.03	0.10
1871	UH	19.29	0.05	0.05	0.01	-0.07	-0.04	0.12
1872	LOT	17.99	0.09	-0.03	-0.01	0.01	-0.06	0.15
1873	UH	17.24	-0.14	-0.05	0.11	0.08		0.25
2146	UH	17.79	-0.07	0.07	0.05	-0.06	0.00	0.14
2207	UH	16.03	0.05	-0.02	-0.03	0.03	-0.03	0.08
2241	UH	15.95	0.11	-0.15	0.01	0.03		0.26

TABLE 2
Photometry of Jovian Trojan Asteroids

2260	UH	17.47	0.03	0.12	-0.09	-0.03	-0.03	0.22
2357	UH	15.93	0.01	0.04	-0.02	-0.03		0.07
2357	LOT	15.96	-0.02	-0.01	-0.01	0.02	0.03	0.05
2363	UH	17.12	0.03	0.03	-0.06	0.01		0.09
2674	LOT	16.54	0.19	-0.23	0.03	0.26	-0.23	0.49
2893	UH	16.62	0.14	-0.03	-0.11	0.00		0.26
2895	UH	17.24	-0.01	-0.04	0.08	-0.02		0.12
2895	LOT	16.73	-0.02	0.05	0.01	-0.01	-0.04	0.09
2920	UH	16.57	0.10	0.06	-0.10	-0.06		0.20
3240	UH	18.06	-0.09	-0.17	0.01	-0.15	0.40	0.57
3317	UH	16.33	0.02	0.01	-0.05	-0.01	0.04	0.09
3451	UH	15.91	-0.10	0.14	0.04	-0.02	-0.06	0.25
3708	UH	17.20	0.01	-0.04	-0.01	0.01	0.02	0.06
3709	UH	17.42	-0.05	-0.04	0.01	-0.05	0.13	0.18
4068	UH	17.41	-0.07	-0.06	0.04	0.04	0.04	0.11
4348	UH	17.09	0.13	0.10	-0.03	-0.01	-0.01	0.16
4489	LOT	17.04	0.08	-0.01	-0.06	-0.01		0.13
4707	LOT	17.81	-0.18	0.16	-0.10	-0.08	0.21	0.40
4708	LOT	17.35	-0.20	0.13	-0.04	0.11		0.33
4709	UH	15.92	-0.05	0.05	0.09	-0.05	-0.06	0.15
4715	LOT	17.13	0.17	-0.23	-0.13	0.23	-0.03	0.46
4722	LOT	17.28	-0.02	0.00	0.01	-0.04	0.05	0.08
4754	LOT	16.95	0.02	0.00	0.01	-0.01	-0.01	0.03
4792	UH	17.85	0.01	0.01	0.01	-0.03		0.05
4792	LOT	17.56	0.17	0.03	-0.10	-0.06	-0.04	0.27
4805	UH	17.73	0.01	0.04	0.04	-0.09		0.14
4827	UH	17.86	0.01	0.07	0.02	-0.06	-0.05	0.13
4828	UH	17.63	0.13	0.11	-0.06	-0.19		0.32
4828	LOT	17.47	0.06	0.00	-0.11	0.06		0.18
4832	LOT	17.55	0.01	0.00	0.01	0.00	-0.02	0.03
4833	UH	17.25	-0.18	0.10	0.13	0.05	-0.10	0.31
4834	UH	17.70	0.06	0.02	-0.02	-0.04	-0.03	0.10
4867	LOT	16.97	0.02	-0.01	-0.02	-0.03	0.04	0.07
5119	UH	17.97	0.07	0.07	-0.02	-0.11		0.18
5233	UH	18.85	0.00	-0.08	0.06	0.02		0.15
5648	UH	17.84	0.06	0.02	-0.03	-0.05		0.11
6002	UH	18.00	0.06	0.03	-0.02	-0.07		0.13
9030	UH	18.20	-0.21	0.06	0.36	-0.08	-0.13	0.57
9142	LOT	18.19	-0.08	0.05	0.04	-0.01	-0.01	0.13
9431	LOT	18.19	0.07	-0.01	-0.12	-0.06	0.13	0.25
9694	UH	17.90	-0.05	-0.16	-0.02	0.08	0.15	0.32
11554	LOT	17.31	0.03	0.00	-0.03	0.00	-0.01	0.06
11668	UH	19.33	-0.05	-0.02	0.14	-0.03	-0.08	0.22
12649	UH	19.64	0.04	0.00	-0.06	0.00	0.02	0.10
13402	UH	19.08	-0.02	0.00	0.00	0.02	0.01	0.04
15527	LOT	18.50	0.05	0.29	-0.13	-0.20		0.49
16667	UH	19.02	-0.11	0.06	0.05	0.01	0.00	0.17
17172	LOT	17.83	0.04	0.03	-0.04	0.00	-0.03	0.07
17365	LOT	17.61	-0.21	0.35	0.05	-0.20		0.56
17419	UH	18.76	-0.03	0.00	0.00	0.02	0.02	0.05
17442	UH	19.39	0.11	0.00	0.06	-0.04	-0.13	0.24
17492	UH	17.70	0.09	0.10	0.03	-0.05	-0.16	0.26
18037	UH	19.22	-0.05	-0.06	-0.03	-0.01	0.15	0.21
18054	UH	18.22	-0.06	0.02	-0.01	-0.01	0.05	0.11
23463	UH	19.15	-0.07	0.01	0.08	-0.04	0.02	0.15
23549	UH	18.90	-0.03	0.02	0.09	0.00	-0.08	0.16
24018	UH	19.19	0.09	0.02	-0.18	-0.11	0.17	0.35
24022	UH	19.79	0.06	-0.08	-0.06	0.08		0.16
24449	UH	19.50	0.13	0.08	-0.17	-0.17	0.13	0.30
24451	UH	18.19	0.04	0.00	0.05	-0.01	-0.07	0.12
24452	UH	19.06	-0.03	0.03	-0.03	0.01	0.01	0.06
24456	UH	19.37	-0.15	0.10	0.13	0.04	-0.11	0.27
24531	LOT	19.72	0.25	-0.07	0.05	0.00	-0.23	0.48
25344	UH	19.22	0.13	0.01	-0.13	-0.11	0.09	0.26
25347	UH	19.23	0.09	0.20	0.04	-0.16	-0.17	0.37
29314	UH	19.44	0.22	0.31	0.21	-0.21	-0.53	0.83
30498	UH	19.59	0.00	-0.07	-0.12	0.10	0.09	0.22
30499	UH	19.76	0.05	-0.03	0.04	-0.07	0.01	0.12
30505	UH	19.02	-0.13	0.15	0.08	-0.22	0.12	0.34
30506	UH	18.78	-0.19	-0.18	-0.02	0.19	0.20	0.39
30704	UH	18.67	-0.08	-0.03	-0.01	0.11		0.19
30942	UH	18.52	0.04	0.02	0.00	-0.02	-0.04	0.08
31806	UH	19.51	0.15	0.07	-0.09	-0.03	-0.10	0.25
31814	UH	19.81	-0.11	0.11	0.23	-0.09	-0.16	0.39
31819	UH	18.90	0.20	0.01	0.00	-0.03	-0.17	0.37
31820	UH	20.06	0.16	0.09	0.05	0.12	-0.40	0.56
32482	LOT	18.68	0.13	-0.14	0.13	0.03	-0.15	0.27

TABLE 2
Photometry of Jovian Trojan Asteroids

32496	UH	18.01	0.01	-0.01	-0.01	0.02	-0.02	0.04
32811	UH	18.43	-0.11	-0.02	0.01	0.05	0.07	0.18
47962	UH	19.59	0.04	-0.05	-0.02	0.00	0.03	0.09
51364	UH	18.49	0.02	0.05	0.04	-0.01	-0.09	0.15
53436	UH	18.40	-0.03	0.02	0.00	0.00	0.01	0.04
55060	LOT	18.85	0.27	-0.09	-0.22	0.03		0.48
55419	LOT	18.68	0.01	-0.22	-0.05	0.20	0.06	0.42
65216	UH	19.67	0.14	-0.02	-0.05	-0.03	-0.03	0.19
67065	UH	18.99	0.08	-0.12	-0.09	0.09	0.04	0.21
69437	UH	19.54	-0.06	0.01	0.01	0.02	0.01	0.08
73677	UH	19.34	0.06	0.03	0.00	-0.02	-0.01	0.08
85798	UH	19.10	-0.08	0.03	0.02	0.03	0.00	0.12
1999 XJ55	UH	19.29	0.04	0.00	-0.03	-0.01		0.06
2000 TG61	UH	19.76	0.01	-0.01	0.00	0.02	-0.03	0.04
2000 SJ350	UH	20.17	-0.20	-0.14	-0.13	0.15	0.08	0.35
2001 QZ113	UH	19.53	-0.02	-0.02	-0.02	0.00	0.05	0.07
2001 XW71	UH	20.24	0.06	-0.03	-0.05	0.17	-0.08	0.24
2001 QQ199	UH	20.51	-0.12	-0.09	0.04	0.05	0.11	0.23
2004 BV84	UH	20.34	0.05	-0.01	0.01	-0.05		0.10
2004 FX147	UH	19.67	0.06	-0.16	-0.13	0.02	0.20	0.36
2005 EJ133	UH	20.15	-0.11	0.01	0.00	0.08	0.01	0.18

[a] Mean R-Band Magnitude
[b] R-Band Magnitude minus Mean R-Band Magnitude
[c] Photometric Range

TABLE 3
Photometry of Jovian Trojan Asteroids

Trojan	$m_R(1,1,0)$[a]	r [AU][b]	Δ [AU][c]	α [degrees][d]	D_e [km][e]	L4/L5
884	8.53	5.66	5.34	9.9	146	L5
1172	8.00	5.68	5.24	9.4	193	L5
1173	9.08	6.02	5.27	6.6	150	L5
1208	8.86	5.69	5.17	9.0	134	L5
1583	9.30	5.33	4.92	10.2	99	L4
1647	11.50	5.20	4.70	10.1	37	L4
1867	8.18	5.34	5.12	10.7	163	L5
1868	9.91	5.50	5.00	9.5	80	L4
1869	12.10	5.49	4.75	7.5	34	L4
1870	10.29	5.42	5.03	10.1	64	L5
1871	11.47	5.46	5.46	10.5	36	L5
1872	10.78	5.51	4.61	4.7	84	L5
1873	9.71	5.11	5.02	11.3	78	L5
2146	9.98	5.69	5.28	9.6	77	L4
2207	8.73	5.05	4.61	10.7	127	L5
2241	8.34	5.17	5.17	11.1	148	L5
2260	9.92	5.39	4.92	9.8	77	L4
2357	8.34	5.29	4.90	10.4	149	L5
2357	8.79	5.29	4.51	7.1	164	L5
2363	9.74	5.24	4.69	9.7	85	L5
2674	9.37	5.17	4.49	8.6	111	L5
2893	8.75	5.56	5.50	10.4	128	L5
2895	9.79	5.25	4.69	9.6	81	L5
2895	9.67	5.24	4.39	6.3	118	L5
2920	9.23	5.25	4.64	9.3	111	L4
3240	10.04	5.92	5.61	9.5	75	L5
3317	8.44	5.78	5.39	9.5	157	L5
3451	8.38	5.44	4.90	9.4	163	L5
3708	9.29	5.93	5.41	8.6	113	L5
3709	9.77	5.58	5.04	9.1	87	L4
4068	9.97	5.33	4.78	9.5	78	L4
4348	9.51	5.49	4.95	9.2	97	L5
4489	9.26	5.54	5.37	10.3	104	L4
4707	10.60	5.53	4.62	4.4	96	L5
4708	10.05	5.34	4.65	8.2	84	L5
4709	8.53	5.30	4.71	9.3	153	L5
4715	9.85	5.30	4.62	8.4	91	L5
4722	10.04	5.44	4.60	6.0	102	L5
4754	10.04	5.22	4.29	4.1	129	L5
4792	10.00	5.69	5.25	9.5	74	L5
4792	10.11	5.68	4.86	6.1	98	L5
4805	10.06	5.46	5.11	10.2	71	L5
4827	10.51	5.08	4.70	10.9	55	L5
4828	10.18	4.96	4.81	11.6	59	L5

TABLE 3
Photometry of Jovian Trojan Asteroids

4828	10.37	4.96	4.40	10.1	63	L5
4832	10.00	5.94	5.03	4.2	128	L5
4833	9.58	5.61	5.07	9.1	95	L4
4834	9.80	5.94	5.38	8.4	91	L4
4867	9.86	5.20	4.43	7.4	97	L5
5119	10.08	5.74	5.30	9.3	72	L5
5233	11.32	5.05	4.92	11.4	35	L5
5648	9.76	5.88	5.62	9.7	82	L5
6002	10.34	5.55	4.97	8.9	66	L5
9030	11.03	5.11	4.46	9.1	49	L5
9142	10.41	5.84	5.27	8.4	70	L5
9431	10.51	5.52	5.17	10.0	59	L4
9694	10.75	5.39	4.51	5.5	78	L4
11554	10.12	5.32	4.53	6.9	90	L5
11668	11.74	5.87	5.04	5.9	47	L4
12649	11.61	5.90	5.58	9.5	36	L5
13402	11.20	5.72	5.35	9.6	43	L5
15527	10.95	5.32	5.01	10.5	47	L4
16667	10.85	6.17	5.88	9.1	54	L5
17172	10.59	5.45	4.61	6.0	80	L5
17365	10.31	5.54	4.69	5.8	92	L5
17419	11.33	5.38	4.81	9.3	43	L5
17442	11.62	5.43	5.35	10.6	34	L5
17492	10.10	5.42	5.07	10.3	70	L5
18037	11.50	5.51	5.21	10.3	37	L5
18054	10.85	5.19	4.74	10.3	50	L5
23463	11.57	5.27	5.05	10.9	34	L5
23549	11.54	5.10	4.76	11.0	35	L5
24018	11.65	5.44	4.95	9.7	36	L5
24022	12.12	5.66	5.12	9.0	30	L5
24449	11.96	5.36	4.94	10.2	30	L5
24451	10.33	5.89	5.39	8.8	70	L5
24452	11.78	5.01	4.63	11.1	31	L5
24456	11.86	5.33	4.90	10.2	31	L5
24531	11.79	5.76	5.57	9.9	33	L4
25344	11.54	5.62	5.11	9.2	39	L5
25347	11.44	5.57	5.32	10.2	38	L5
29314	11.84	5.46	5.02	9.9	32	L5
30498	11.78	5.70	5.33	9.7	34	L5
30499	12.16	5.32	5.06	10.7	26	L5
30505	11.60	5.32	4.76	9.5	37	L5
30506	11.06	5.43	5.24	10.6	44	L5
30704	11.20	5.34	4.85	9.8	43	L5
30942	11.20	5.17	4.64	10.0	43	L5
31806	11.73	5.67	5.29	9.7	34	L5
31814	12.16	5.65	5.10	8.9	30	L5
31819	11.65	5.14	4.57	9.8	36	L5
31820	12.46	5.50	5.03	9.6	25	L5
32482	11.36	5.26	4.66	9.2	42	L5
32496	10.30	5.63	5.17	9.5	68	L5
32811	11.14	5.00	4.64	11.2	41	L5
47962	12.04	5.54	4.95	8.9	32	L5
51364	11.42	4.95	4.34	9.9	39	L5
53436	11.36	5.21	4.35	6.4	54	L4
55060	11.41	5.34	4.83	9.6	40	L5
55419	11.12	5.51	4.98	9.1	47	L5
65216	12.49	5.44	4.54	5.2	36	L4
67065	12.02	5.20	4.30	5.3	44	L4
69437	11.89	5.55	5.10	9.7	32	L5
73677	11.99	5.27	4.70	9.6	31	L5
85798	11.89	5.45	4.57	5.6	45	L4
1999 XJ55	12.21	5.29	4.42	6.0	38	L4
2000 TG61	12.23	5.47	4.92	9.2	28	L5
2000 SJ350	12.55	5.44	5.03	10.0	23	L5
2001 QZ113	11.98	5.39	4.98	10.2	30	L5
2001 XW71	12.71	5.51	4.89	8.7	23	L5
2001 QQ199	12.59	6.36	5.48	4.6	37	L5
2004 BV84	12.95	5.37	4.74	8.8	21	L5
2004 FX147	12.61	5.25	4.39	6.0	31	L4
2005 EJ133	12.72	5.39	4.80	9.1	23	L5

[a] Absolute Magnitude (see Equation 1)
[b] Heliocentric Distance
[c] Geocentric Distance
[d] Phase Angle
[e] Effective Diameter (see Equation 2)

Raw data frames were bias subtracted, then flat fielded using a master flat field produced from median filtering dithered images of the sky taken at dusk and dawn. Landolt (1992) standard star fields were imaged and mea-

sured to convert the instrumental magnitudes to an absolute magnitude scale. An aperture radius of eight pixels was consistently used throughout the observations for images taken on both telescopes. Median sky values were determined using an adjacent annulus around the aperture having an outer radius of 20 pixels. The reason for similar aperture and sky annulus size on both telescopes, despite differing pixel scales was because of the significantly worse seeing conditions at Lulin (see Table 1). For the sparse sampling survey, two images were taken in each setting and then averaged to obtain the brightness measurement. The photometric uncertainties are small ($\leq$ 0.02 mag.) compared to the photometric variability that is the subject of interest and so we have ignored these uncertainties in our presentation of the data. For the densely sampled lightcurves, errors for each observation were calculated using Poisson statistics. The instrumental magnitude of the asteroid in each image was subtracted from the brightness of a nearby field star. The field star was chosen to be persistent in all five observations and helped reduce photometric errors by providing a correction for weather variations occuring throughout the night. Images in which the asteroid was affected by proximity to a field star were rejected and resulted in some Trojans having only four measurements of brightness rather than five.

3. RESULTS

Tables 2 and 3 contain results of the sparsely sampled lightcurve survey. In Table 2, the average R band magnitude, $\overline{m_R}$ is listed, along with the independent measurements of the asteroid's brightness, expressed as deviations from the mean magnitude. The last column shows the maximum deviation measured, which gives a lower limit to the photometric range of each asteroid. Table 3 contains the absolute magnitude, $m_R(1,1,0)$, which is defined as the magnitude an object would have if placed at heliocentric (r) and geocentric (Δ) distances of 1 AU, and at a phase angle of $\alpha = 0$ degrees. The conversion between the apparent magnitude, m_R and absolute magnitude, $m_R(1,1,0)$ is

$$m_R(1,1,0) = m_R - 5log(r\Delta) - \beta\alpha, \qquad (1)$$

where β is the phase coefficient for which we used a value of 0.04 magnitudes per degree for the low albedo Trojan asteroids (Bowell et al. 1989). Also listed in Table 3 is an estimate of the equivalent circular diameter, D_e which was calculated using (Russell 1916)

$$m_R(1,1,0) = m_\odot - 2.5\log\left[\frac{pD_e^2}{4\times 2.25\times 10^{16}}\right]. \qquad (2)$$

Here, p is the geometric albedo, for which a value of 0.04 was used throughout (Fernandez, Sheppard & Jewitt 2003) and $m_\odot$ = -27.1 is the apparent red magnitude of the sun (Cox 2000).

Figures 4 shows the distribution of photometric ranges shown by the Trojan asteroids in the sparsely-sampled lightcurve survey. For comparison, Figure 5 shows the photometric range distributions of both the Trojan and Main Belt asteroids with diameters between 70-km and 150-km (Main Belt asteroid data taken from

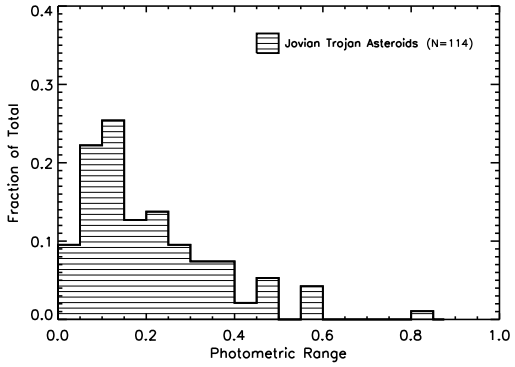

FIG. 4.— Histogram of the distribution of photometric ranges found from sparse-sampled observations of 114 Jovian Trojan asteroids.

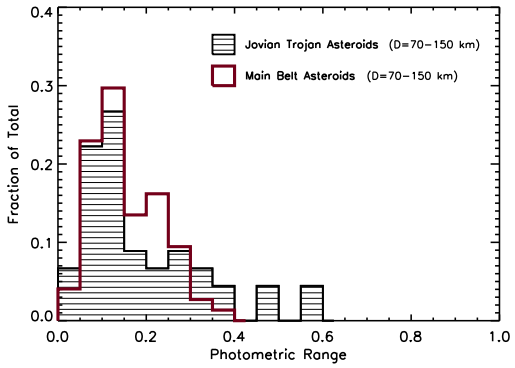

FIG. 5.— Histogram of the photometric ranges of Jovian Trojan asteroids and Main Belt asteroids with diameters between 70-km and 150-km. Data for Main Belt asteroids taken from Barucci et al. (2002).

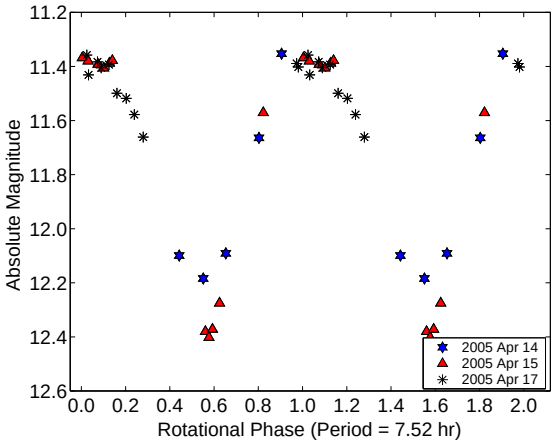

FIG. 6.— Absolute magnitude (calculated from equation 1) of Trojan asteroid (29314) in April 2005. Data are phased to a single-peaked lightcurve period of 7.52 hours.

Barucci et al. (2002)). Figure 5 reveals that a larger fraction of Trojan asteroids have photometric ranges larger than Main Belt asteroids, similar to previous studies by Hartmann et al. (1988). A Kolmogorov-Smirnov statistical test found a 32.1% probability that the two distributions are drawn from the same parent distribution.

Trojan asteroids (17365) and (29314) showed the largest photometric ranges in the sparsely-sampled photometry, with 0.56 $\pm$ 0.02 magnitudes and 0.83 $\pm$ 0.03

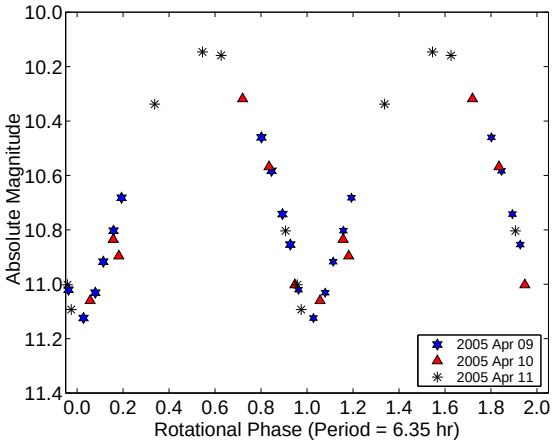

FIG. 7.— Absolute magnitude (see equation 1) of Trojan asteroid (17365) in April 2005. Data are phased to a single-peaked lightcurve period of 6.35 hours.

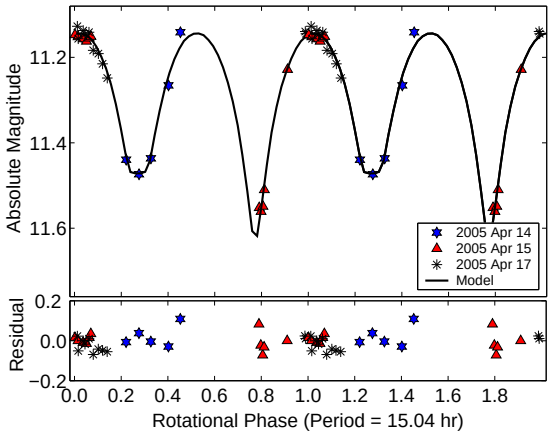

FIG. 8.— Absolute magnitude (see equation 1) of Trojan asteroid (29314) in April 2005. Data phased to a double-peaked lightcurve period of 15.04 hours. Best fit Roche binary equilibrium model is overplotted.

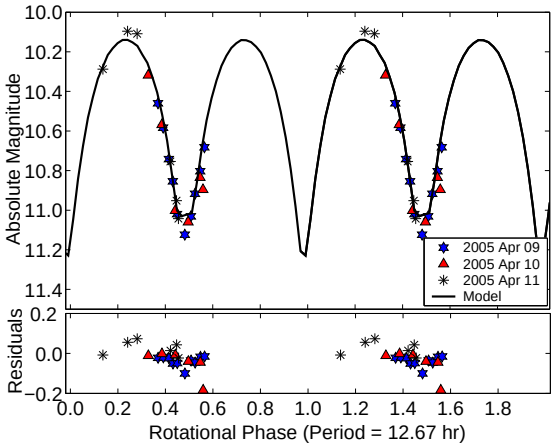

FIG. 9.— Absolute magnitude (see equation 1) of Trojan asteroid (17365) in April 2005. Data phased to a double-peaked lightcurve period of 12.67 hours. Best fit Roche binary equilibrium model is overplotted.

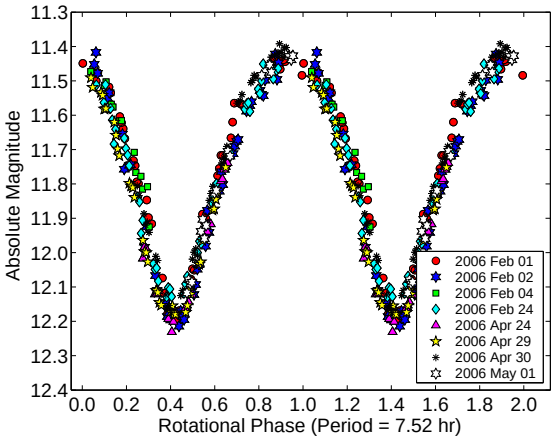

FIG. 10.— Absolute magnitude (see equation 1) of Trojan asteroid (29314) between February and May 2006. Data are phased to a single-peaked lightcurve period of 7.52 hours.

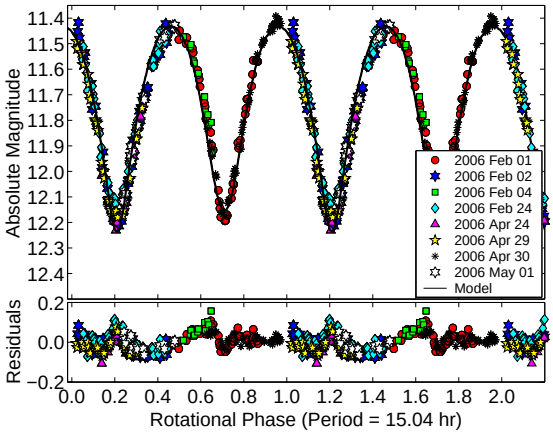

FIG. 11.— Absolute magnitude (see equation 1) of Trojan asteroid (29314) between February and May 2006. Data are phased to a double-peaked lightcurve period of 15.04 hours. Best fit Roche binary equilibrium model is overplotted.

magnitudes, respectively (see Table 2). Follow-up observations to obtain densely sampled optical lightcurves for both Trojan asteroids were taken using the University of Hawaii 2.2-m telescope between 2005 April 9th and 17th. We were unable to complete the observations due to bad weather coupled with the fact the asteroids were quickly setting. We were however, able to confirm the large photometric ranges to motivate further study of these Trojan asteroids (see Figures 6 through 9). In our first dense light curve study, in 2005, asteroid (17365) had a photometric range of 0.98 ± 0.02 magnitudes, centered at a mean of 10.64 ± 0.01 magnitudes, while asteroid (29314) had a peak-to-peak lightcurve amplitude of 1.05 ± 0.03 centered on 11.89 ± 0.02 magnitudes.

To complete the lightcurve study, we continued optical observations of both candidate contact binary asteroids in 2006. Figures 10 through 13 show the results of the photometric observations. In 2006, asteroid (17365) showed a photometric range of 0.81 ± 0.02 magnitudes, centered at a mean absolute magnitude of 10.76 ± 0.01. Asteroid (29314) shows a peak-to-peak amplitude of 0.86 ± 0.03 magnitudes, with a mean absolute magnitude of 11.80 ± 0.02.

The phase dispersion minimization (PDM) method (Stellingwerf 1978) was used to determine possible ro-

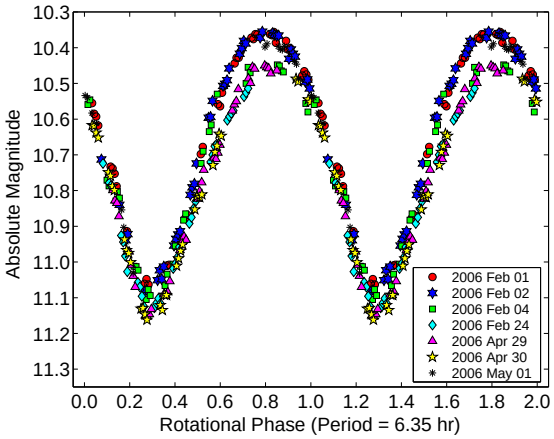

FIG. 12.— Absolute magnitude (see equation 1) of Trojan asteroid (17365) between February and May 2006. Data are phased to a single-peaked lightcurve period of 6.35 hours.

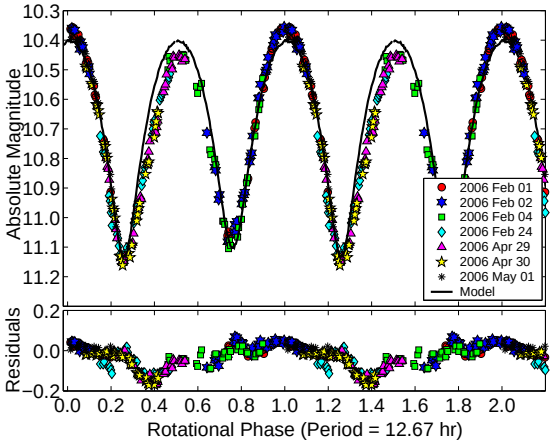

FIG. 13.— Absolute magnitude (see equation 1) of Trojan asteroid (17365) between February and May 2006. Data are phased to a double-peaked lightcurve period of 12.67 hours. Best fit Roche binary equilibrium model is overplotted.

tation periods for each asteroid. Figures 14 and 15 show plots of Θ, which characterizes the dispersion in the data phased to a given period (see Stellingwerf (1978) for more information). The most likely rotation periods correspond to the smallest values of theta. Several periods appeared to minimize theta, but when used to phase the data, the results were not persuasive lightcurves. In fact, only two periods per asteroid produced convincing lightcurve results. For Trojan (29314), minima consistent with the data occur at periods of 0.3133 ± 0.0003 days (7.518 ± 0.007 hr), and a double-peaked period of 0.6265 ± 0.0003 days (15.035 ± 0.007 hr). Asteroid (17365) shows a single-peaked lightcurve period of 0.2640 ± 0.0004 days (6.336 ± 0.009 hr) and double-peaked period of 0.52799 ± 0.0008 days (12.672 ± 0.019 hr).

While both the single-peaked and double-peaked periods produce good fits for Trojan asteroid (29314), the double-peaked lightcurve is more convincing. The lightcurve of (29314) shows subtle differences in the shapes of the two minima, which is obvious by the spread in the data when phased to the single-peaked period (see Figure 10 and 11). Asteroid (17365) shows a more obvious double-peaked lightcurve (see Figures 12 and 13) with maxima of different shapes. The maxima of (17365) differ by 0.10 ± 0.01 magnitudes while the minima differ

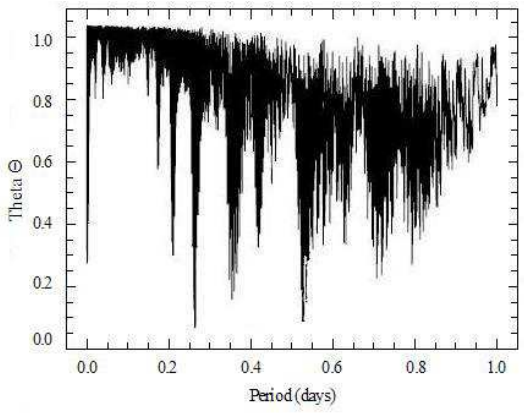

FIG. 14.— Phase Dispersion Minimization (PDM) plot for Trojan asteroid (17365) showing Θ versus period. Probable periods are at minimum Θ values: 0.2640 ± 0.0004 days and 0.52799 ± 0.0008 days.

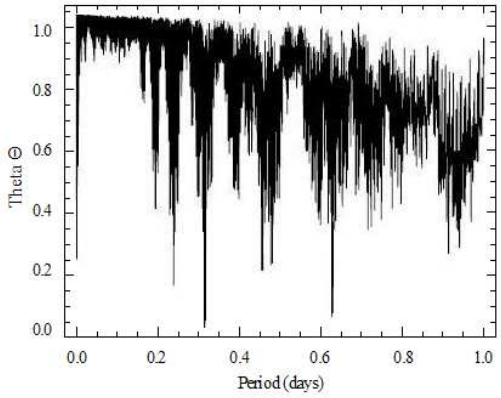

FIG. 15.— Phase Dispersion Minimization (PDM) plot for Trojan asteroid (29314) showing Θ versus period. Probable periods minimize Θ: 0.3133 ± 0.0003 days and 0.6265 ± 0.0003 days.

by 0.06 ± 0.01 magnitudes.

3.1. *Candidate Contact Binary Asteroids*

Trojan asteroids (17365) and (29314) show strong evidence of being contact binaries. Both asteroids reveal photometric ranges greater than 0.9 magnitudes, sufficiently long rotation periods (< 2 rotations per day) and lightcurve profiles (qualitatively similar to 624 Hektor) containing U-shaped maxima and V-shaped minima. Here, we speculate about all possible explanations for the brightness variations in the lightcurve observations of these Trojan asteroids, including albedo variations, elongated shapes or binarity (Dunlap & Gehrels 1969; Cook 1971; Hartmann & Cruikshank 1978; Weidenschilling 1980).

Surface albedo contrasts provide a possible but unconvincing explanation for the large brightness variations of the Trojans. Amongst Solar system objects, only Iapetus, a satellite of Saturn, shows strong spatial albedo variations which account for its large lightcurve amplitude. However, Iapetus' synchronous rotation about Saturn plays a large role in producing the dichotomous behaviour of the satellite (Cook & Franklin 1970) and this circumstance is not relevant in the context of the Trojan

asteroids. Amongst previously studied asteroids, double-peaked lightcurves are almost always caused by rotational variations in the projected area, and reflect the elongated shapes of the bodies. While albedo contrasts cannot be formally ruled out, we feel that they are an unlikely cause of the observed brightness variations.

Increasing evidence suggests asteroids have little or no internal strength, probably as a result of impacts that disrupt but do not disperse the object (Farinella et al. 1981; Pravec, Harris, & Michalowski 2002). The Trojan asteroids have undergone a collisional history that is either similar to that of the main-belt asteroids (Marzari et al. 1997) or perhaps even more intense (Davis et al. 2002; Barucci et al. 2002), making it highly probable that they, too, are gravity dominated "rubble piles", strengthless or nearly so in tension (Farinella et al. 1981). Studies have found that only the smallest main-belt asteroids, with diameters less than 0.15-km, have sufficient internal strength to overcome gravity (Pravec, Harris, & Michalowski 2002). Figure 5 from Pravec, Harris, & Michalowski (2002) shows observations of decreasing maximum spin rate with increasing lightcurve amplitude (a proxy for elongation) of near-earth asteroids. This observation indicates a lack of fast rotating elongated bodies, which implies that asteroids larger than ~ 0.15-km are structurally weak and lack the tensile strength to withstand high rotation rates without becoming unstable and flying apart. Also evident in Figure 5 (Pravec, Harris, & Michalowski 2002) is the tendency of fast rotators to have spheroidal shapes, an indicator of gravity-dominated bodies which do not possess the internal strength to resist gravity. Collectively, the observations point to asteroids being bodies of negligible strength, whose shapes are dominated by rotation and gravity.

Rotation rates must lie between 4 and 6 rotations per day in order for rotational elongation of a structurally weak body to be maintained. This is the range for which Jacobi ellipsoids are possible figures of equilibrium (Leone et al. 1984; Farinella & Zappalà 1997). If the rotation rate was much higher than 6 rotations per day, the body would fall apart, while at a much lower rotation rate, the body would adopt a spherical figure of equilibrium. In 2005, both asteroids (17365) and (29314) showed photometric variations larger than 0.9 magnitudes, above the threshold for rotational instability in a structurally weak body. Additionally, both asteroids have double-peaked lightcurve periods that are too slow to cause sufficient rotational elongation. Both observations indicate that rotationally-induced elongation is an insufficient explanation for the brightness variations of these Trojan asteroids.

We are therefore left with the strong possibility that Trojan asteroids (29314) and (17365) are contact binaries. Figure 16 is a plot of rotation periods and photometric ranges of several well studied Kuiper Belt objects and main-belt asteroids. It is divided into three main regions: Region A spans the photometric ranges that can be explained by albedo variations, elongation or binarity of an asteroid. Region B represents the characteristics explained by albedo variations or rotational elongation of an object, while variations in region C can only be explained by binary asteroids. Both Trojan asteroids lie well within Region C, alongside contact binaries 216

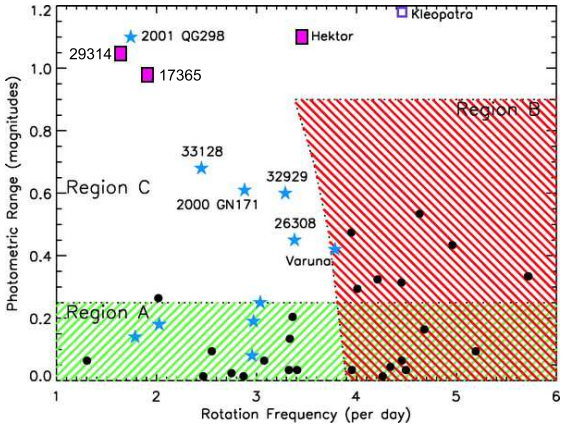

FIG. 16.— Modification of Figure 5 from Sheppard & Jewitt, 2004 (originally taken from Leone et al. 1984) to include contact binary candidates (17365) and (29314). Stars represent Kuiper Belt objects, black circles are main-belt asteroids with diameters larger than 50-km and pink squares are the candidate binary Trojans (17365), (29314) and 624 Hektor. Region A includes all objects whose photometric range could be caused by albedo, elongation or binarity. Region B contains objects that are likely to be rotationally elongated. Only binaries are expected in Region C.

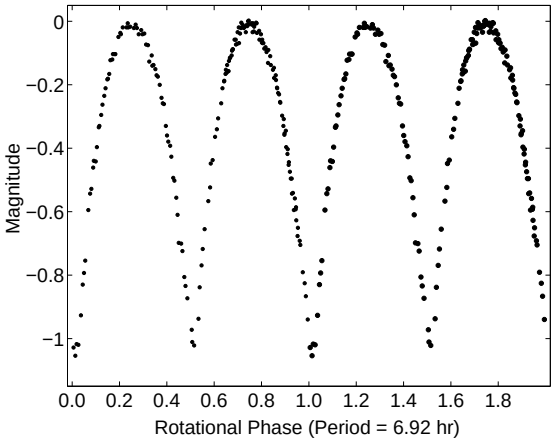

FIG. 17.— Lightcurve of 624 Hektor in April 1968, taken from Dunlap & Gehrels (1969). Note the similarities between lightcurves of (29314), (17365) and 624 Hektor.

Kleopatra, 624 Hektor and 2001 QG_{298}, contributing to their suspected binary nature.

The lightcurve of a contact binary is expected to show U-shaped or spread out maxima and V-shaped or notched minima, as shown by the lightcurves of 2001 QG_{298} (see Sheppard & Jewitt (2004)) and 624 Hektor (see Figure 17). These characteristic lightcurve profiles are unlike the distinctive "notched" profile expected for wide, eclipsing binaries which remain flat for the majority of the orbit, and contain sharp dips during the relatively short eclipsing events. The photometric observations of Trojan asteroids (29314) and (17365) are consistent with lightcurve profiles expected of very close or contact binary systems.

624 Hektor was recently discovered to possess a satellite of diameter 15-km using Keck Laser Guide Star Adaptive Optics (Marchis et al. 2006b), but an independent density estimate derived from the orbital motion of this satellite has not yet been published. Additionally, the imaging observations of 624 Hektor indicate that its primary component has a double-lobed nature. Similarities are obvious between the lightcurves of 624 Hektor,

(17365) and (29314) (see Figures 11, 13 and 17) and consistent with our interpretation that the latter two asteroids are contact binaries.

We used equilibrium models of Roche binaries to determine how well the photometric observations of (17365) and (29314) could be matched by theoretical lightcurves of contact binary systems. A Roche binary consists of a pair of homogeneous bodies in hydrostatic equilibrium orbiting each other. A strength of this modeling is the ability to estimate densities for the asteroids without knowing the sizes of the binary components. The exact shapes and rotation rates of the Roche binaries were calculated using the mathematical description presented in Leone et al. (1984) (see also Chandrasekhar (1987)). Binary configurations were calculated for secondary to primary mass ratios from $q = 0.25$ to $q = 1.00$ in steps of 0.01. For each value q, Equations 1 to 3 of Leone et al. (1984) were solved simultaneously to find possible shapes and orbital frequencies for the primary. The same equations were then solved using mass ratio $q' = 1/q$ to calculate the shapes and orbital rates for the secondary. Finally, valid binaries are uniquely selected by matching pairs (q,1/q) with the same orbital frequency. This procedure is described in detail in Leone et al. (1984) and Lacerda & Jewitt (2007).

The models were ray-traced using publicly available software POV-Ray (http://www.povray.org), but the surface scattering routine of POV-Ray was rewritten to allow better control of the scattering function. The scattering law used here was first implemented by Kaasalainen, Torppa, & Muinonen (2001). It linearly combines single (Lommel-Seeliger) and multiple (Lambert) scattering terms using a parameter k (Takahashi & Ip 2004), which varies from 0 to 1. The resulting reflectance function is

$$r \propto (1-k)\,\frac{\mu_0}{\mu_0+\mu} + k\,\mu_0 \qquad (3)$$

where μ_0 and μ are the cosines of the incidence and emission angles. When $k = 0$, only single scattering is present, while $k = 1$ simulates pure multiple scattering of light off the surface of the binaries. All binary configurations were raytraced for k between 0 and 1 in steps of 0.1. Two viewing geometries were modelled, at aspect angles of 75 and 90 deg (equator-on). The aspect angle lies between the line of sight of the observations and the rotation axis of the body. Simulated illumination angles were chosen to match the phase angles at the time the data were taken. In total, nearly 50000 models were computed for comparison with the data.

Observations of (17365) and (29314) were simultaneously fitted for the different viewing orientations in 2005 and 2006 to find the best shape interpretation for the asteroids. We assumed that the objects were viewed equatorially in 2005, thus producing the larger photometric range in the discovery epoch data. This assumption was encouraged by the fact that an aspect angle of 75 degrees (rather than 90 degrees) produced a better fit with the 2006 observations (see Figures 10 and 12).

Figures 8, 9, 11 and 13 show the best-fit models overlaying lightcurve data, with residuals plotted underneath. Best fit models were found by minimizing chi-squared. Small deviations (~ 0.1 magnitudes) from the binary model are evident for both asteroids, but are negligible compared with the total range of the observations, the more important parameter. Presumably, the deviations are caused by irregularities on the surface of the asteroids, which were not included in the simple binary model, but without which the asteroids would be considered odd. The ability of the models to simultaneously fit two epochs of photometric observations lends strong support to the idea that we observed contact binary asteroids over two years at different viewing geometries.

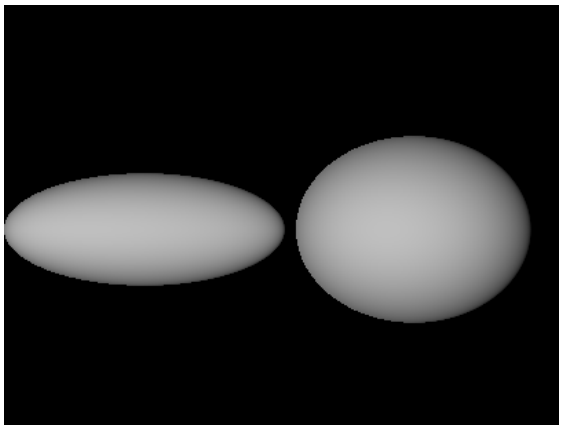

FIG. 18.— Shape interpretation of Trojan asteroid (29314) from Roche binary equilibrium models.

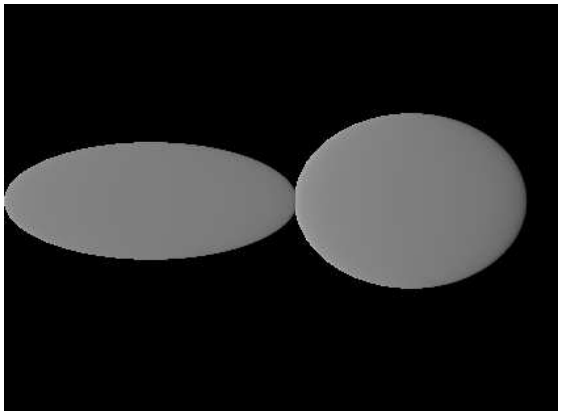

FIG. 19.— Shape interpretation of Trojan asteroid (17365) from Roche binary equilibrium models.

Figures 18 and 19 show the shapes derived from the binary models for (17365) and (29314). Orbital periods combined with shape information allowed us to estimate the densities of the asteroids. The components of our model of asteroid (29314) were found to have a mass ratio of $0.4^{+0.5}_{-0.1}$ and a density of 590^{+40}_{-80} kg/m^3, while our best model of asteroid (17365) has a mass ratio of $0.6^{+0.2}_{-0.1}$ and density of 780^{+50}_{-80} kg/m^3. These low densities suggest porous asteroid interiors. If (29314) and (17365) have a rock/ice composition similar to the moons of Jupiter, (29314) would have a porosity of $\sim 64\%$, while (17365) would have a smaller porosity of 50% (see Figure 3 from Marchis et al. (2006a)). If (17365) and (29314) were composed purely of water ice, their porosities would be 15% and 35%, respectively (Marchis et al. 2006a). This pure water ice composition is unrealistic, however. It is interesting to note that our low density measurements are consistent with 617 Patroclus (Marchis et al. 2006a).

Among the Trojans, only 624 Hektor is known to have

a comparable lightcurve amplitude, making (29314) and (17265) the 2nd and 3rd known Trojans to show such large rotational variations. Lightcurve analysis suffers from the notorious non-uniqueness problem, which arises from the ability to reproduce any lightcurve with a complicated pattern of surface markings and shapes. Our interpretation is not unique, but is the simplest, most plausible explanation for the behaviour of the Trojan asteroids.

4. DISCUSSION: BINARY FRACTION

Following the method outlined in Sheppard & Jewitt (2004) to account for the geometrical circumstances of the observations, we were able to estimate the fraction of contact binary systems among the Jovian Trojan asteroids. This method uses two very crude approximations. In the first approximation, the binary system is simplified to be an elongated, rectangular object with dimensions a ≥ b = c, having a lightcurve amplitude as follows:

$$\Delta m = 2.5 \log \left\{ \frac{1 + \tan\theta}{\frac{b}{a} + \tan\theta} \right\}. \quad (4)$$

The range of lightcurve amplitudes used to identify contact binary asteroids is 0.9 to 1.2 magnitudes. For the maximum amplitude of 1.2 magnitudes and viewing angle of $\theta = 0°$, an axis ratio of $\frac{a}{b} = 3$ is calculated from Equation 4. Using this axis ratio and the minimum expected amplitude of 0.9 magnitudes, a viewing angle of 10° was determined. Therefore, the range of lightcurve amplitudes expected for a contact binary asteroid would only be observed if the Earth lies within 10° of the equator of the asteroid. The probability that the Earth would lie within 10° of the equator of a randomly oriented asteroid is $P(\theta \leqslant 10°) = 0.17$. We found two suspected contact binary asteroids in our sample of 114 Trojan asteroids, so the fraction of contact binary Jovian Trojan asteroids is approximately $\frac{2}{114(0.17)} = 10$ %.

A second approximation uses an ellipsoid shape to represent the contact binary asteroid, again having dimensions a ≥ b = c, and having a lightcurve amplitude expressed by the following:

$$\Delta m = 2.5 \log \left(\frac{a}{b}\right) - 1.25 \log \left\{ \left[\left(\frac{a}{b}\right)^2 - 1 \right] \sin^2\theta + 1 \right\}. \quad (5)$$

Using the axis ratio of $\frac{a}{b} = 3$, in order to observe photometric ranges between 0.9 and 1.2 magnitudes, the Earth must lie within 17° of the equator of the ellipsoidal asteroid. The probability of a randomly oriented object having this geometrical orientation relative to the observer is $P(\theta \leqslant 17°) = 0.29$, implying a contact binary fraction of $\frac{2}{114(0.29)} = 6$ %.

We conclude that the fraction of contact binary Trojan asteroids is ∼6% to ∼10%. This is a lower limit to the actual fraction as some of the objects not found in the survey sample to have large amplitudes might in fact have them because the sparse sampling method is not 100% efficient. The existence of likely contact binary 624 Hektor separately suggests that the binary fraction is high.

Binaries with equal-sized components are rare in the main-belt (the frequency of large main-belt binaries is ∼ 2% (Richardson & Walsh 2006)) and have yet to be observed in the near-earth asteroid population. However, they are abundant in the observed binary Kuiper Belt population, where the fraction lies between 10% and 20% (Sheppard & Jewitt 2004). The results of this study show that there are three Jovian Trojan asteroids that reside in Region C. The observations tend to suggest a closer relationship between the binary populations of the Kuiper Belt and the Trojan clouds. This correlation could signify similar binary formation mechanisms in the two populations. This is an interesting connection considering that in one model of formation, the Trojans are actually captured Kuiper Belt objects (Morbidelli et al. 2005). However, it is clear that the total binary fractions in the Kuiper Belt and in the Trojans needs to be more tightly constrained before conclusions can be made.

The contact binaries detected were skewed towards those with components of comparable sizes, which are capable of producing photometric ranges ≥ 0.9 magnitudes. For mass ratios ≪ 1, sparse sampling would more likely miss the eclipsing event and the photometric range would be ≤ 0.9 magnitudes and would not attract our attention. The method was strongly dependent on geometrical circumstances, and only binaries viewed edge-on or almost equatorially would be detected in our survey. Additionally, sparse sampling is only able to put lower limits on the photometric range of an asteroid, making the binary fraction a lower limit estimate. Only binaries with sufficiently short orbital periods (optimally between 6 to 12 hour rotation periods) would be detected, so wide binaries were not accounted for in this study. Therefore, again the measured binary fraction is a strong lower limit to the actual fraction and is suggestive of a significant binary population among the Trojan clouds.

Our project is a pilot study for the much larger scale Pan-STARRS, which will detect every object with a red magnitude brighter than 24^{th} magnitude. It is estimated that approximately 10^5 Jovian Trojans exist with red magnitudes lower than 24, all of which will be detected using Pan-STARRS (Jewitt 2003; Ďurech et al. 2006). Our results suggest that Pan-STARRS will reveal between 6000 and 10,000 contact binary systems among the Trojan clouds.

TABLE 4
Likely Contact Binary Trojans

Asteroid	$\bar{m}(1,1,0)$[a]	D_e [km][b]	P [hr]	Δm[c]	ρ [kg/m^3]
(17365)	10.76	92	12.672	0.98	780
(29314)	11.80	32	15.035	1.05	590
624 Hektor	7.37	350 × 210	6.921	1.10	2200

[a] Mean Absolute Magnitude (see Equation 1)
[b] Effective Diameter (see Equation 2)
[c] Maximum Photometric Range

5. SUMMARY

Sparsely sampled lightcurve measurements were used to statistically study the photometric variations of 114 Jovian Trojan asteroids. Objects with large photometric ranges were targeted for follow-up in this survey, and are considered as candidate contact binary systems.

1. The sparse sampling technique successfully confirmed known photometric ranges of both 944 Hi-

dalgo (0.58 ± 0.02 magnitudes) and 2674 Pandarus (0.50 ± 0.01 magnitudes).

2. Two of the 114 observed Trojans, asteroids (17365) and (29314), were found to show photometric ranges larger than expected for rotationally deformed equilibrium figures, and were targeted for dense follow-up lightcurve observations. The resulting ranges (0.98 ± 0.02 mag and 1.05 ± 0.03 mag, respectively) and long rotation periods (12.672 ± 0.019 hr and 15.035 ± 0.007 hr) of these two Trojans are consistent with a contact binary structure for each object.

3. Roche binary models give densities of 780^{+50}_{-80} kg/m^3 for asteroid (17365) and 590^{+40}_{-80} kg/m^3 for asteroid (29314), suggestive of porous interiors.

4. If (17365) and (29314) are indeed contact binaries, then we estimate from our survey that the binary fraction of the Jovian Trojans is $\sim$6% to 10% or more. The total binary fraction (including both wide and close pairs) must be higher.

We thank John Dvorak, Daniel Birchall, Dave Brennan and Ian Renaud-Kim for operating the UH telescope and Henry Hsieh for assisting with the observations both in Taiwan and Honolulu. We are grateful for the assistance and expertise of the Lulin Observatory staff, in particular Wen-Ping Chen, Chung-Ming Ko and HC Lin. Support for this work by a grant to D.J. from NASA's Origins Program is greatly appreciated.

REFERENCES

Astakhov, S.A., Lee, E.A., Farrelly, D. 2005, MNRAS, 360, 401
Barucci, M.A., Cruikshank, D.P., Mottola, S., Lazzarin, M. 2002, in Asteroids III, ed. W.F. Bottke Jr., A. Cellino, P. Paolicchi & R. P. Binzel (Tucson: Univ. Arizona Press), 273
Belton, M., Champman, C., Thomas, P., Davies, M., Greenberg, R., Klaasen, K., Byrnes, D., D'Amario, L., Synnott, S., Merline, W., Petit, J.M., Storrs, A., Zellner, B. 1995, Nature, 374, 785
Binzel, R.P., & Sauter, L.M. 1992, Icarus, 95, 222-238
Bowell, E., Hapke, B., Domingue, D., Lumme, K., Peltoniemi, J., and Harris, A.W. 1989, in Asteroids II, ed. R.P. Binzel, T. Gehrels & M.S. Matthews (Tucson: Univ. Arizona Press), 524
Cellino, A., Pannunzio, R., Zappalá, V., Farinella, P., Paolicchi,P. 1985, A&A, 144, 355
Chandrasekhar, S. 1987, Ellipsoidal Figures of Equilibrium (New York: Dover)
Chapman, C.R., Veverka, J., Thomas, P.C., Klaasen, K., Belton, M.J.S. Harch, A., McEwen, A., Johnson, T.V., Helfenstein, P., Davies, M.E., Merline, W.J., Denk, T. 1995, Nature, 374, 783
Cook, A.F., Franklin, F.A. 1970, Icarus, 13, 282
Cook, A.F. 1971, in Physical Studies of Minor Planets, ed. T. Gehrels, 155
Cox, A.N., 2000, in Allen's Astrophysical Quantities, (New York: Springer-Verlag), 341
Davis, D.R., Durda, D.D., Marzari, F., Campo B.A., Gil-Hutton, R. 2002, in Asteroids III, ed. W.F. Bottke Jr., A. Cellino, P. Paolicchi, & R. P. Binzel (Tucson: Univ. Arizona Press), 545
Dunlap, J. L., Gehrels, T. 1969, AJ, 74, 796
Ďurech, J., Grav, T., Jedicke, R., Denneau, L., & Kaasalainen, M. 2005, Earth Moon and Planets, 97, 179
Farinella, P., Paolicchi, P., Tedesco, E.F., Zappalá, V. 1981, Icarus, 46, 114
Farinella, P., Zappalà, V. 1997, Advances in Space Research, 19, 181
Fernández, Y.R., Sheppard, S.S., Jewitt, D.C. 2003, AJ, 126, 1563
Funato, Y., Makino, J., Hut, P., Kokubo, E., Kinoshita, D. 2004, Nature, 427, 518
Goldreich, P., Lithwick, Y., Sari, R. 2002, Nature, 420, 643
Harris, A.W., Lagerkvist, C.I., Zappalá, V., Warner, B.D. Minor Planet Lightcurve Parameters, Jan 15, 2006. http://cfa-www.harvard.edu/iau/lists/LightcurveDat.html
Hartmann, W.K., Cruikshank, D.P. 1978, Icarus, 36, 353
Hartmann, W.K., Binzel, R. P., Tholen, D.J., Cruikshank, D.P., Goguen, J. 1988, Icarus, 73, 487
Holsapple, K. A. 2004, Icarus, 172, 272
Ivezic, Z., et al. 2001, AJ, 122, 2749
Jewitt, D.C., Trujillo, C.A., & Luu, J.X. 2000, AJ, 120, 1140
Jewitt, D.C., 2003, Earth, Moon, and Planets, 92, 465
Jewitt, D. C., Sheppard, S., Porco, C. 2004, in Jupiter: The planet, satellites and magnetosphere. ed. Bagenal, F., Dowling, T.E., McKinnon, W.B. Vol. 1 (Cambridge University Press), 263
Kaasalainen, M., Torppa, J., Muinonen, K. 2001, Icarus, 153, 37
Kaasalainen, M., Torppa, J., Piironen, J. 2002, A&A, 383, L19
Lacerda, P., Jewitt, D. 2007, AJ,133, 1393
Landolt, A.U. 1992, AJ, 104, 340
Leone, G., Paolicchi, P., Farinella, P., Zappalái, V. 1984, A&A, 140, 265
Marchis, F., et al. 2006a Nature, 439, 565
Marchis, F. Wong, M. H., Berthier, J., Descamps, P., Hestroffer, D., Vachier, F., Le Mignant, D., Keck Observatory, W.M., de Pater, I. 2006b, IAU Circ., 8732, 1
Marzari, F., Farinella, P., Davis, D.R., Scholl, H., Campo B.A. 1997, Icarus, 125, 39
Merline, W.J., et al. 2001, IAU Circ., 7741, 2
Morbidelli, A., Levison, H. F., Tsiganis, K., Gomes, R. 2005, Nature, 435, 462
Pravec, P., Harris, A.W., Michalowski, T. 2002, in Asteroids III, ed. W.F. Bottke Jr., A. Cellino, P. Paolicchi, & R. P. Binzel (Tucson: Univ. Arizona Press), 113
Richardson, D.C., & Walsh, K.J. 2006, Annual Review of Earth and Planetary Sciences, 34, 47
Russell, H.N. 1916, AJ, 43, 173
Stellingwerf, R.F. 1978. ApJ, 224, 953
Sheppard, S. & Jewitt, D.C. 2004, AJ, 127, 3023
Takahashi, S., & Ip, W. H. 2004, PASJ, 56, 1099
Weidenschilling, S. J. 1980, Icarus, 44, 807
Weidenschilling, S. J. 1989, in Asteroids II, ed. R. P. Binzel, T. Gehrels, M.S. Matthews (Tucson: Univ. Arizona Press), 643
Weidenschilling, S.J. 2002, Icarus, 160, 212
Wisniewski, W.Z., Michalowski, T.M., Harris, A.W., McMillan, R.S. 1997, Icarus, 126, 395
Yoshida, F., & Nakamura, T. 2005, AJ, 130, 2900